

# Maximum Likelihood Particle Tracking in Turbulent Flows via Sparse Optimization

Griffin M. Kearney<sup>1,2,\*</sup>; Kasey M. Laurent<sup>1,†</sup>; Makan Fardad<sup>1,‡</sup>

<sup>1</sup>*Syracuse University, Syracuse, NY 13244*  
<sup>2</sup>*OpB Data Insights LLC, Syracuse, NY 13224*

February 27, 2026

---

## Abstract

Lagrangian particle tracking is essential for characterizing turbulent flows, but inferring particle acceleration from inherently noisy position data remains a significant challenge. Fluid particles in turbulence experience extreme, intermittent accelerations, resulting in heavy-tailed probability density functions (PDFs) that deviate strongly from Gaussian predictions. Existing filtering techniques, such as Gaussian kernels and penalized B-splines, implicitly assume Gaussian-distributed jerk, thereby penalizing sparse, high-magnitude acceleration changes and artificially suppressing the intermittent tails. In this work, we develop a novel maximum likelihood estimation (MLE) framework that explicitly accounts for this non-Gaussian intermittency. By formulating a modified Gaussian process to model the random incremental forcing, we introduce a sparse optimization scheme utilizing a convex  $\ell_1$ -relaxation. To overcome the numerical stiffness associated with high-order difference operators, the problem is efficiently solved using an iteratively reweighted least squares (IRLS) algorithm. The proposed filter is evaluated against direct numerical simulation (DNS) data of homogeneous, isotropic turbulence ( $\text{Re}_\lambda \approx 310$ ). Results demonstrate that the IRLS approach consistently outperforms state-of-the-art discrete MLE, continuous MLE, and B-spline methods, yielding systematic reductions in root-mean-squared error (RMSE) across position, velocity, and acceleration. Most importantly, the proposed framework succeeds in better recovering the heavy-tailed statistical structure of both acceleration and acceleration differences (jerk) across temporal scales, preserving the physical intermittency characteristic of high-Reynolds-number turbulent flows that baseline methods severely attenuate.

## 1 Introduction

Understanding the dynamics of fluid particles in turbulence is essential for characterizing mixing, dispersion, and energy transfer across scales. Turbulence consists of spatially and temporally localized regions of intense velocity gradients, where fluid particles are subject to extreme accelerations as they pass through coherent structures such as vortex tubes. These interactions result in intermittent acceleration statistics, where probability density functions (PDFs) consist of heavy tails that deviate significantly from Gaussian

---

\*gkearneyengineering@gmail.com

†klaurent@syr.edu

‡makan@syr.edu

predictions. Experimental Lagrangian particle tracking techniques have made it possible to capture detailed particle trajectories, but acceleration must be inferred from inherently noisy position data, requiring filtering methods that inevitably embed assumptions about the nature of the particle motion. To accurately estimate accelerations from noisy position data, filtering must be informed by the physics of turbulent fluctuations to avoid biasing acceleration statistics.

Acceleration PDFs of fluid particles in turbulence exhibit a peak at zero and heavy tails, deviating strongly from a Gaussian distribution. Voth et al. (2002) reported experimental one-component acceleration PDFs with kurtosis values exceeding 40, dependent on the Reynolds number. Mordant et al. (2004) extended measurements to probabilities as low as  $10^{-7}$  and observed persistent heavy tails in the PDF of accelerations, extending beyond 50 standard deviations. The existence of heavy tails implies rare, intense acceleration events, due to strong intermittency inherent to small-scale turbulence. Extreme accelerations are produced when fluid particles encounter intense, small-scale flow structures which impart sudden and large forces on the particle (Bentkamp et al. 2019).

Early efforts to estimate acceleration from noisy particle tracks obtained from experiments primarily focused on noise suppression without explicitly incorporating flow physics. Early particle tracking studies often used low-order polynomial fits over a sliding window of a few points to compute velocities and accelerations (Voth et al. 2002; Ayyalasomayajula et al. 2006; Lüthi et al. 2005). The polynomial order and window length must be carefully chosen; if it is too low, the curvature of the trajectory cannot be captured, and if it is too high, the filter overfits and results in nonphysical oscillations. Another common technique is Gaussian kernel convolution, introduced by Mordant et al. (2004). The need to convolve with a kernel over multiple points means that very short particle tracks cannot be filtered. Short tracks frequently belong to fast-moving particles, which inherently experience larger accelerations (Sawford et al. 2003). Omitting these trajectories leads to a selection bias in which extreme events are filtered out, causing a suppression of the acceleration PDF tails. This bias can be mitigated by oversampling; however, achieving the necessary sample rates (100 samples/Kolmogorov time scale, or tens to thousands of frames per second (Voth et al. 2002)) is technologically challenging, especially while maintaining a large measurement volume.

In recent years, more sophisticated smoothing techniques have been developed to improve acceleration estimates from noisy position data. Most notable is the TrackFit (or FlowFit in the Eulerian case) algorithm, described in Gesemann (2015), which uses penalized B-spline fitting. In this approach, each particle trajectory is approximated by a cubic B-spline, whose shape is determined by minimizing a cost function that penalizes deviations from data as well as excessive curvature. Gesemann (2021) showed that B-spline fitting reduces the sensitivity of acceleration statistics to filter length and resolves smaller-scale features compared to the Gaussian kernel method. Lawson et al. (2018) found that with this B-spline approach, the estimated acceleration variance and kurtosis plateau to stable values for a wide range of filter parameters whereas the Gaussian kernel approach produced results that varied significantly. The TrackFit approach effectively imposes a penalty on the third derivative of the trajectory, discouraging large values in jerk. In Kearney et al. (2024), we developed a Bayesian Maximum Likelihood Estimation (MLE) framework that incorporates joint process and measurement randomness. The method explicitly models the jerk of the fluid particle as a Gaussian random process rather than treating it implicitly, and we found the observed performance to be comparable to that of the B-splines. In parallel, we developed a related MLE framework for general data systems (Kearney and Fardad 2024), that likewise models jerk as a Gaussian process, to construct optimal spline functions and denoising conditions which yield continuous-time smooth trajectories. The framework uses a control theoretic approach which enables the rigorous modeling of both stochastic process dynamics and measurements, making it well suited for the fluid particle tracking problem considered in the present work.

Observed deviations from Gaussianity have led to the development of stochastic models that explicitly incorporate intermittency. Kolmogorov 1941 theory assumes homogeneous, isotropic self-similar turbulence with no intermittency (Kolmogorov 1941), while the refined similarity hypothesis introduces a fluctuating

small-scale dissipation rate (Kolmogorov 1962). Assuming the local dissipation is log-normal, the acceleration PDF becomes a mixture of Gaussians, yielding heavy-tailed distributions consistent with experiments (Mordant et al. 2004). However, this framework fails to capture high-order statistics (Frisch and Kolmogorov 1995). The Sawford model (Sawford 1991) provided an early stochastic description of velocity and acceleration using a second-order autoregressive process, but its Gaussian acceleration assumption prevents reproduction of intermittency. To overcome this limitation, a number of other Lagrangian models have been developed. Beck (2001) modeled fluctuating acceleration variance with a  $\chi^2$  distribution, producing power-law tails but a divergent fourth moment inconsistent with experiments (Mordant et al. 2004). Later extensions in Beck (2003) adopted a log-normal variance, producing better agreement with observed flatness and tail behavior for acceleration PDFs. Similarly, Reynolds (2003) incorporated a fluctuating dissipation variable within a Markovian framework, assuming Gaussian acceleration conditioned on local dissipation in accordance with refined similarity theory, successfully reproducing heavy tails and Reynolds-number dependence consistent with experiments (La Porta et al. 2001; Voth et al. 2002). Motivated by DNS evidence that conditional acceleration remains intermittent, Lamorgese et al. (2007) introduced a conditionally cubic-Gaussian extension that better captures PDF shape and tails. Multifractal cascade approaches have also been applied, with Arimitsu and Arimitsu (2004) deriving acceleration PDFs via generalized entropy maximization and Chevillard and Meneveau (2006) predicting Reynolds-dependent acceleration statistics consistent with DNS and experiments.

In general, the developed models for Lagrangian particle motion in turbulence indicate that the jerk will be non-Gaussian, contradicting the assumed Gaussian distribution for the TrackFit filter and MLE filters. As a result, occasional large spikes in acceleration change will be penalized and under-represented in data processed with TrackFit. In this paper, we develop and evaluate an improved MLE framework for recovering particle acceleration from noisy position data without imposing a Gaussian-distributed jerk. This filtering approach allows for greater flexibility in capturing the rapid, intermittent changes in acceleration that are characteristic of turbulent flows. By formulating the problem in this framework, we can incorporate non-Gaussian models for acceleration differences. This approach offers a way to evaluate the role of prior assumptions in trajectory filtering and provides a foundation for more physically consistent acceleration estimates, improving our ability to analyze Lagrangian turbulence from experimental data.

The current gap lies in the disconnect between physics and filtering practice. While particle velocity differences and acceleration in turbulent flows have been extensively characterized, the behavior of the acceleration differences and jerk has received relatively little attention. Jerk reflects how rapidly the forces acting on a fluid particle change over time, revealing how particles interact with fine-scale structures in the flow. Heavy tails in PDF of jerk imply large, abrupt changes in acceleration (for example, a particle suddenly entering or exiting a strong vortex filament). Existing models imply this behavior. For the Sawford model (Sawford 1991), jerk is not well-defined, due to the white-noise forcing of acceleration. While an explicit PDF for jerk is not given for later models in Beck (2001, 2003); Reynolds (2003); Lamorgese et al. (2007), one can infer that jerk inherits intermittency, and large jerks are expected when there are sharp changes in the local dissipation rate. Arimitsu and Arimitsu (2004) proposed a multifractal approach grounded in generalized entropy maximization. They explicitly derive the acceleration PDF, which closely matches experimental data (Mordant et al. 2004). This model tends to perform better than other models in reproducing the core of the acceleration distribution, whereas log-normal models tend to overestimate. Additionally, the approach described in Chevillard and Meneveau (2006) produces fluid velocity that is infinitely differentiable at finite Reynolds numbers; the model predicts that jerk will also display intermittent fluctuations.

The remainder of this paper is organized as follows: Section 2 details the mathematical formulation of the maximum likelihood estimation framework, introducing the modified Gaussian process model for intermittent jerk and the subsequent convex relaxation of the optimization problem. Section 3 outlines the methodology, including the numerical implementation of the iteratively reweighted least squares (IRLS) solver and the error quantification metrics applied to the synthetic turbulent trajectory data. Section 4 presents

the results and discussion, comparing the proposed IRLS filter’s performance against existing state-of-the-art filtering techniques. Finally, Section 5 offers concluding remarks and highlights avenues for future work, including the potential for real-time state estimation and establishing rigorous links between optimization hyperparameters and physical flow constants.

## 2 Technical Development

In this section we will standardize the maximum likelihood analysis presented in our past work (Kearney et al. 2024) by developing the general problem in terms of modern optimization in Section 2.1. This treatment provides a sufficiently general framework for application to many interesting particle tracking data systems, including those with non-Gaussian randomness.

In Section 2.2, we develop a specific realization of the general framework by modifying the assumed statistical structure of the process dynamics. Here, we challenge the notion that standard Gaussian distributions are accurate representations of the random incremental forcing, or jerk, on a fluid particle.

The optimization problem derived in Section 2.3 using the nonstandard distribution is nonconvex, and thus it is difficult to analyze in its original form. In Section 2.4 we apply relaxation techniques to derive convex approximations which are easily solvable using standard convex optimization techniques. The solution of the convex relaxation is discussed further when results are presented in Section 4.

### 2.1 A Standard Maximum Likelihood Framework

In previous work (Kearney et al. 2024), we developed a maximum likelihood data filtering scheme using Bayesian arguments. However, the approach is better standardized using optimization-theoretic treatments in which the framework is stated using optimization objectives and constraints. The objective of the scheme is a measure of the total probability, which depends on both the distribution of process randomness and the measurement error. The constraints are used to enforce the dynamics underlying the data system as well as the structure of the measurement errors.

We consider particle trajectories that are discrete time series of length  $T$ , where  $T$  denotes the total number of samples. We define  $x$  to be the  $T$ -dimensional vector representing the true trajectory of the particle in a single positional dimension, absent measurement error, and  $y$  to be the  $T_m$ -dimensional vector representing noisy measurements of  $x$ . Here  $T_m$  denotes the number of discrete measurements gathered to perform the smoothing, and in direct sampling schemes we have  $T_m = T$ . We define  $v$  to be a random vector-valued variable of dimension  $T_d$ .  $T_d$  denotes the number of discrete points at which the dynamics are computed; for instance, when applying standard finite difference equations  $T_d < T$  since central differencing cannot be applied outright at the edges of the vector  $x$ . The vector  $v$  represents the process noise and is used to model uncertainty in the dynamics. Similarly, we define  $w$  to be a random vector-valued variable of dimension  $T_m$  that represents the measurement noise and which is used to model uncertainty in observations. The random processes  $v$  and  $w$  are the core of the system likelihood as they are non-deterministic. We denote their probability density functions as  $\rho_v(v)$  and  $\rho_w(w)$ , respectively. Furthermore, we assume that  $v$  and  $w$  are independent random variables so that the joint probability density function ( $\rho(v, w)$ ) is the product, given by

$$\rho(v, w) = \rho_v(v)\rho_w(w). \quad (1)$$

The natural logarithm is a monotonic function, so without loss of generality we use

$$J(v, w) = \log \rho(v, w) = \log \rho_v(v) + \log \rho_w(w), \quad (2)$$

as the maximization objective of our framework, and we next move to consider constraints. We assume that

the dynamics are modeled using a stochastic process of the form

$$Ax = v, \quad (3)$$

where  $A$  is a matrix of dimension  $T_d \times T$ ; “the dynamics matrix”. The model described in (3) is useful as it can be used to describe the discretized form of any linear differential equation. Similarly, we assume that noisy observations are of the form

$$y = Bx + w, \quad (4)$$

where  $B$  is a matrix of dimension  $T_m \times T$ ; “the observation matrix”. Equations (3) and (4) comprise the constraints of the optimization problem, enforcing the problem dynamics and measurement system in the solution. The general problem in our framework is written

$$\begin{aligned} \max_{x, v, w} \quad & J(v, w) \\ \text{s.t.} \quad & Ax = v \\ & y = Bx + w. \end{aligned} \quad (5)$$

The framework provided in (5) is populated by specifying the dynamics matrix  $A$ , observation matrix  $B$ , and the probability distributions  $\rho_v$  and  $\rho_w$  of  $v$  and  $w$ , respectively. We will consider directly measured systems where  $B = I$ , the  $T \times T$  identity matrix, in the remainder of this work. In the next section we examine the TURB-Lagr data to demonstrate that  $v$  exhibits a nonstandard distribution. The distribution takes the form of a modified Gaussian distribution, one which is described by a Gaussian distribution with additional atomic probability weight at the point  $v = 0$ . The hybrid discrete-continuous nature of this type of modified distribution necessitates additional considerations when incorporating it in our optimization framework as it does not permit a continuous probability density function.

## 2.2 Modified Gaussian Distribution Modeling in Turbulent Data

In (5) we prescribe distributions that govern the process randomness ( $v$ ) and the measurement error ( $w$ ) which ultimately determine the structure of the objective  $J$ . A well-established approach, and one that we utilized in our previous work, is to assume that both sources of uncertainty were Gaussian in nature, which leads to a quadratic program. However, despite our imposing these processes within a third order system (e.g. Gaussian jerk), we observed that this leads to muted acceleration distributions in smoothed trajectories; a persistent problem among existing methods. Our prior approach showed improved performance over standard convolution smoothing as developed in (Mordant et al. 2001) and performed comparably, if not slightly better, than B-spline type methods (Gesemann 2015). Importantly, our method was built upon physical first principles that we have standardized in the prior section. The comparable performance in B-spline methods rely on empirical motivations. We emphasized in our initial work that our framework enables us to incorporate general modifications in a way that other methods cannot. We proceed to do so here by developing a *modified Gaussian process* (MGP) smoother using our approach.

We maintain the standard Gaussian model for the measurement noise  $w$  as before, but consider a modified variant in lieu of a standard Gaussian to model  $v$ . We again utilize a third order system in which the equation  $Ax = v$  is prescribed as a system of finite differences that describe jerk estimates which will be elaborated upon in Section 2.3. The MGP is developed conditionally, to describe the treatment let us begin by assuming  $v_k$  is a random *modified Gaussian variable* (MGV) corresponding to such a process and which constitutes the  $k$ -th component of the vector  $v$ . The variable  $v_k$  is assumed to take the value 0 with probability  $p_0 \in [0, 1]$  and otherwise it takes a value governed by the distribution  $N(0, \sigma_v^2)$ . For convenience we denote this modified distribution as  $\tilde{N}(p_0, 0, \sigma_v^2)$ .

Under this definition, the system dynamics can be viewed as “stubborn Gaussian”: it has some base likelihood  $p_0$  in which nothing happens (e.g.  $v = 0$ ), inducing intermittency in the dynamics. When a non-zero jerk is present in the system (with likelihood  $1 - p_0$ ), then the non-zero value is taken from a Gaussian distribution. In essence we are adding extra weight to the 0 likelihood and this in turn enables us to increase  $\sigma_v$  to accommodate increased volatility when force-changing events occur. We treat  $v$  as a vector with identical independently distributed (IID) components, each of which is a MGW.

### 2.3 Modeling of the Maximum Likelihood Estimator

Modeling the maximum likelihood estimator boils down to quantifying the likelihood of the observation of such a vector  $v$ . We utilize a simple central difference approximation of a third order system in (3) using the matrix

$$A = \frac{1}{\Delta t^3} \begin{bmatrix} -1 & 3 & -3 & 1 & 0 & \dots & 0 \\ 0 & -1 & 3 & -3 & 1 & \dots & 0 \\ \vdots & \ddots & \ddots & \ddots & \ddots & \ddots & \vdots \\ 0 & \dots & 0 & -1 & 3 & -3 & 1 \end{bmatrix} \quad (6)$$

where  $\Delta t$  denotes the sampling period. This matrix is of dimension  $T - 3 \times T$  which requires that  $v$  is of dimension  $T - 3$ . Consider  $v$  with  $0 \leq n \leq T - 3$  non-zero components, corresponding to a non-zero index set  $\mathcal{N} \subseteq \{1, 2, \dots, T - 3\}$ ; or in other words  $|\mathcal{N}| = n$ . Under the IID assumption the  $n$  nontrivial components are governed by the distribution

$$\rho_v(v | \mathcal{N}) = \left( \frac{1}{\sqrt{2\pi}\sigma_v} \right)^n e^{-\frac{\|v\|^2}{2\sigma_v^2}}, \quad (7)$$

where the full norm of the vector  $v$  is used in the exponent since the norm of the full vector is equal to the norm of its non-zero components, trivially. The probability of this non-zero index set is given by

$$p(\mathcal{N}) = \left( p_0 \right)^{T-3-n} \left( 1 - p_0 \right)^n = \left( p_0 \right)^{T-3} \left( \frac{1 - p_0}{p_0} \right)^n. \quad (8)$$

Strictly speaking, it is possible for  $\text{card}(v)$  (the cardinality of  $v$ ) to be less than  $n$ ; the distribution  $N(0, \sigma_v^2)$  has support at the value 0. We treat this as pathological, for it occurs with probability zero. We therefore assume  $n = \text{card}(v)$  which enables us to write the joint distribution

$$\rho_v(v \cap \mathcal{N}) = p(\mathcal{N})\rho_v(v | \mathcal{N}) = (p_0)^{T-3} \left( \frac{1 - p_0}{\sqrt{2\pi}\sigma_v p_0} \right)^{\text{card}(v)} e^{-\frac{\|v\|^2}{2\sigma_v^2}}. \quad (9)$$

As in our prior work, we assume that the measurement errors are IID Gaussian random variables with zero mean and variance  $\sigma_w^2$ . This yields the distribution

$$\rho_w(w) = \left( \frac{1}{\sqrt{2\pi}\sigma_w} \right)^T e^{-\frac{\|w\|^2}{2\sigma_w^2}}. \quad (10)$$

We assume that the process and measurement randomness are independent so that the joint distribution is given by the product of (9) and (10). We use this product, and after discarding immaterial constant factors, it yields the objective  $J(v, w)$

$$J(v, w) = -\frac{\|v\|^2}{2\sigma_v^2} - \frac{\|w\|^2}{2\sigma_w^2} - \log\left( \frac{\sqrt{2\pi}\sigma_v p_0}{1 - p_0} \right)^{\text{card}(v)}. \quad (11)$$

Finally, after absorbing a negative sign to exchange the max for a min, this yields the maximum likelihood estimator given by the optimization framework:

$$\begin{aligned} \min_{x,v,w} \quad & \frac{\|v\|^2}{2\sigma_v^2} + \frac{\|w\|^2}{2\sigma_w^2} + \log\left(\frac{\sqrt{2\pi}\sigma_v p_0}{1-p_0}\right) \text{card}(v) \\ \text{s.t.} \quad & Ax = v \\ & y = x + w. \end{aligned} \quad (12)$$

Problem (12) is not convex in general due to the cardinality term of the objective. Solving this system is therefore non-trivial but convex relaxations do exist which enable efficient computation of practically relevant solutions.

A key parameter within our new problem is the cardinality coefficient, given by

$$\gamma = \log\left(\frac{\sqrt{2\pi}\sigma_v p_0}{1-p_0}\right). \quad (13)$$

If  $\gamma < 0$  then the cardinality no longer induces a penalty and instead rewards non-zero components in  $v$ . When this is the case, a standard quadratic programming solver (convex) is applied since the cardinality term can be omitted; this is equivalent to the discrete MLE solver we developed in our prior work. We focus on the more interesting case when  $\gamma > 0$ , which is equivalent to the condition

$$\frac{\sqrt{2\pi}\sigma_v p_0}{1-p_0} > 1. \quad (14)$$

Equation (14) defines a relationship between  $\sigma_v$  and  $p_0$  that determines when the trade-off between volatility in the non-zero stochastic dynamics and the “stubbornness” of the modified process becomes meaningful. In the next section we will describe how the 1-norm can be used to relax the nonconvex optimization problem (12) when (14) is satisfied.

## 2.4 Finding Solutions of the Maximum Likelihood Estimator

Were it not for the existence of the cardinality function in its objective (or equivalently, were  $\gamma \leq 0$ ) the optimization problem

$$\begin{aligned} \min_{x,v,w} \quad & \frac{1}{2\sigma_v^2} \|v\|^2 + \frac{1}{2\sigma_w^2} \|w\|^2 + \gamma \text{card}(v) \\ \text{s.t.} \quad & Ax = v \\ & y = x + w. \end{aligned} \quad (15)$$

would be a convex quadratic program, which can be solved in closed-form. The inclusion of  $\text{card}(v)$  in (15) penalizes the number of non-zero entries in  $v$  and, as  $\gamma$  increases, renders evermore sparse solutions for  $v$ . However, it also renders the optimization problem combinatorial in nature and intractable in general.

It is well-known (Boyd and Vandenberghe 2004) that the 1-norm (also referred to as the  $\ell_1$ -norm) serves as a convex relaxation of  $\text{card}(\cdot)$  while preserving much of its sparsity-promoting properties. We thus

consider the optimization problem

$$\begin{aligned} \min_{x,v,w} \quad & \frac{1}{2\sigma_v^2} \|v\|^2 + \frac{1}{2\sigma_w^2} \|w\|^2 + \gamma \|v\|_1 \\ \text{s.t.} \quad & Ax = v \\ & y = x + w. \end{aligned} \tag{16}$$

which is convex and therefore can be solved efficiently (numerically) for very large problems. The optimization problem posed in (16) belongs to a class of  $\ell_1$ -regularized least squares problems, widely known in signal processing as basis pursuit denoising (Chen et al. 1998) and in statistics as lasso (Tibshirani 1996). While the problem is convex, the non-differentiability of the  $\ell_1$ -norm at the origin precludes the use of standard gradient descent methods. Two families of iterative algorithms are typically employed to solve such large-scale non-smooth problems: splitting methods and reweighted least squares.

Splitting methods, most notably the Alternating Direction Method of Multipliers (ADMM), introduce auxiliary variables to decouple the non-smooth sparsity penalty from the smooth data fidelity term (Boyd et al. 2011). This separation allows for efficient closed-form updates of each component. However, in the context of Lagrangian particle tracking, the dynamic matrix  $A$  represents a high-order difference operator divided by a small time step  $\Delta t$ . This structure frequently results in systems with high condition numbers leading to numerical stiffness. In such stiff regimes, first-order splitting methods like ADMM often exhibit slow convergence tails or stalling behavior, failing to resolve the high-amplitude, sparse events that characterize the heavy tails of the probability distribution.

An alternative approach is the Iteratively Reweighted Least Squares (IRLS) algorithm. IRLS handles the non-smooth objective by approximating the  $\ell_1$ -norm with a weighted  $\ell_2$ -norm, transforming the problem into a sequence of smooth, quadratic minimization sub-problems. The primary advantage of this formulation is that each sub-problem is a linear system that can be solved using direct matrix factorization methods (e.g., Cholesky or LDL decomposition). Unlike first-order methods, direct solvers are inherently robust to ill-conditioning, ensuring high-precision solutions even when the dynamic constraints are numerically stiff. Given our requirement to accurately recover extreme acceleration events without smoothing bias, we adopt the IRLS framework for the remainder of this work.

### 3 Methods

We evaluated the proposed filter on 6,000 simulated three-dimensional fluid particle trajectories, each consisting of 1,800 time steps, obtained from a direct numerical simulation (DNS) of homogeneous, isotropic turbulence with  $\text{Re}_\lambda \approx 310$ . The simulated trajectories were drawn from the TURB-Lagr database (Biferale et al. 2024), and include particle position, velocity, acceleration, and local velocity gradient information. The time step between stored samples is  $\Delta t \approx \tau_\eta/153$ .

Synthetic position noise was added to DNS particle trajectories prior to filtering. We used each of the simulated particle trajectories as a ground truth ( $x$ ) and applied simulated zero-mean Gaussian position errors ( $w$ ) to generate “noisy” measurements ( $y$ ). For each trajectory we apply the smoothing scheme described by (12) using the convex relaxation presented in (16). We simulated the measurement error as white noise with standard deviation  $\sigma_w = 0.0063$  for all experiments. The smoothing scheme and simulation procedure operate on each spatial component of the particle trajectory independently.

#### 3.1 Solver Implementation

The optimization problem presented in (16) involves a non-smooth  $\ell_1$ -regularization term and is characterized by significant numerical stiffness. This stiffness arises from the large disparity between the weights of the data

fidelity term (governed by the small measurement error  $\sigma_w$ ) and the sparsity inducing term. While first-order splitting methods, such as the Alternating Direction Method of Multipliers (ADMM), are commonly used for such problems, they frequently exhibit slow convergence or stalling behavior in stiff parameter regimes, potentially smoothing out the extreme events (heavy tails) of interest.

To address these challenges, we employ an iteratively reweighted least squares (IRLS) algorithm (Daubechies et al. 2010). This approach transforms the non-smooth optimization problem into a sequence of smooth, weighted least-squares sub-problems. Unlike splitting methods, IRLS allows for the use of direct linear solvers, which are robust to ill-conditioning and ensure high-precision convergence.

At each iteration  $k$ , we approximate the objective function in (16) by a quadratic form. The non-smooth penalty  $\gamma\|v\|_1$  is replaced by a weighted  $\ell_2$ -norm term  $\frac{1}{2}v^T\Omega^{(k)}v$ , where  $\Omega^{(k)}$  is a diagonal weighting matrix updated based on the solution from the previous iteration. To consistently approximate the combined  $\ell_2$  and  $\ell_1$  penalties on the jerk  $v$ , the diagonal entries are defined as:

$$\Omega_{ii}^{(k)} = \frac{1}{\sigma_v^2} + \frac{2\gamma}{|v_i^{(k-1)}| + \epsilon}, \quad (17)$$

where  $v_i^{(k-1)}$  is the  $i$ -th component of the jerk estimated at iteration  $k-1$ , and  $\epsilon$  is a small regularization constant (set to  $10^{-6}$ ) effectively acting as a smoothing parameter to prevent numerical instability when  $v_i$  approaches zero.

Substituting this approximation into the objective, the update step for the trajectory  $x$  at iteration  $k$  becomes the solution to a weighted least squares problem:

$$x^{(k)} = \underset{x}{\operatorname{argmin}} \left( \frac{1}{2\sigma_w^2} \|y - x\|_2^2 + \frac{1}{2} (Ax)^T \Omega^{(k)} (Ax) \right). \quad (18)$$

The optimality condition for (18) yields the following linear system:

$$\left( \frac{1}{\sigma_w^2} I + A^T \Omega^{(k)} A \right) x^{(k)} = \frac{1}{\sigma_w^2} y. \quad (19)$$

Since  $A$  represents a finite difference operator, the matrix  $A^T \Omega^{(k)} A$  retains a sparse, banded structure. This structure permits the system to be solved efficiently using direct sparse Cholesky factorization with a computational complexity of  $\mathcal{O}(T)$ . The algorithm iterates between updating the weights via (17) and solving the system (19) until convergence. This direct solver approach avoids the convergence issues of iterative splitting methods in stiff regimes, allowing for the accurate recovery of the heavy-tailed acceleration distributions characteristic of high-Reynolds-number turbulence.

### 3.2 Error Quantification

The TURB-Lagr simulation data provide ground-truth trajectory positions, velocities, and accelerations, enabling direct quantitative evaluation. We use  $x$  to denote the true (one-dimensional) discrete position,  $u$  for the true discrete velocity, and  $a$  for the true discrete acceleration over the time interval. Quantities marked with a hat denote filter estimates obtained after operating on noisy measurements. The proposed filters operate component-wise and the resulting three data streams are collected to form the discrete time vectors  $\hat{x}$ ,  $\hat{u}$ , and  $\hat{a}$ , respectively. These filtered discrete-time vector quantities are used to compute the error  $e(\cdot)$ . For a given trajectory, the instantaneous reconstruction error is defined at each discrete time  $t$  via:

$$e_{\hat{x}}(t) = \hat{x}(t) - x(t), \quad (20)$$

where (20) is defined on the reconstructed position  $\hat{x}$ , but is used analogously for velocity and acceleration.

To quantify the overall reconstruction accuracy for an individual trajectory, we compute the root-mean-squared error (RMSE),

$$E(\hat{x}) = \sqrt{\frac{1}{T} \sum_{t=1}^T \|e_{\hat{x}}(t)\|^2}, \quad (21)$$

where again (21) is illustrated on the position, but is applied to the velocity and acceleration identically.

Section 4.1 evaluates the distributions of the position, velocity, and acceleration RMSE across a set of candidate filtering schemes. Because the IRLS filter depends on two tunable parameters, the analysis also quantifies parameter sensitivity and establishes a practical tuning strategy that does not rely on knowledge of the true trajectory.

## 4 Results and Discussion

We demonstrate the improved performance of the proposed IRLS filter through a comparative study with other state-of-the-art methods. In our preliminary work (Kearney et al. 2024), we demonstrated that the discrete MLE filter without intermittency considerably outperformed baseline Gaussian smoothing (Mordant et al. 2001). However, our standard Gaussian MLE smoother performance was comparable to the B-spline approach (Gesemann 2015). Accordingly, we use the standard Gaussian MLE filter, B-spline smoothing and an additional MLE-based spline (referred to as the continuous MLE filter) that uses the general MLE spline construction approach (Kearney and Fardad 2024). The MLE-based splines are constructed using standard Gaussian process noise and a third-order (i.e. jerk) continuous system consistent with the model used in the MLE filter and the proposed method. For all filtering methods, we determined the filter parameters through an exhaustive search, seeking to minimize the average RMSE.

Critical to this study, we evaluate the recovery of turbulent flow physics by examining the statistics of the Lagrangian acceleration and acceleration differences. Since the filter operates on position, acceleration is derived via second-order central finite differences of the smoothed position estimates. We compute the probability density functions (PDFs) of the acceleration components, normalized by their respective standard deviations. These distributions are plotted on semi-logarithmic axes to explicitly inspect the behavior of the tails. The primary criterion for success of the IRLS filter is its ability to better reproduce the heavy, non-Gaussian tails observed in the DNS ground truth. This is an artifact of the sparse high-jerk events, rather than the parabolic shape characteristic of Gaussian smoothing artifacts.

### 4.1 Filter Tuning and Sensitivity

The efficacy of the proposed IRLS filter relies on the selection of two hyperparameters: the process noise standard deviation  $\sigma_v$ , which governs the assumed volatility of the jerk, and the sparsity penalty parameter  $\gamma$  as defined in (13), which controls the strength of the  $\ell_1$  regularization. The measurement noise level  $\sigma_w$  was held fixed throughout all experiments to be representative of a simulated experimental setup.

To determine an optimal tuning configuration, we employed a hierarchical grid-search strategy over the parameter space  $(\sigma_v, \gamma)$  using a representative subset of 200 trajectories for computational efficiency. We evaluated the filter performance using a dual-objective criterion in which we quantified both position and acceleration errors of the smoothed trajectory versus the known true trajectories taken directly from the TURB-Lagr dataset. Across wide variations in  $\sigma_v$ , the resulting error landscapes exhibited minimal variation in comparison to the strong gradients observed along the  $\gamma$  direction. In other words, the sparsity penalty almost entirely governs the reconstruction quality, whereas the assumed process noise width contributes only marginally. We provide the tuning surfaces developed in the process of conducting this study in Appendix A.

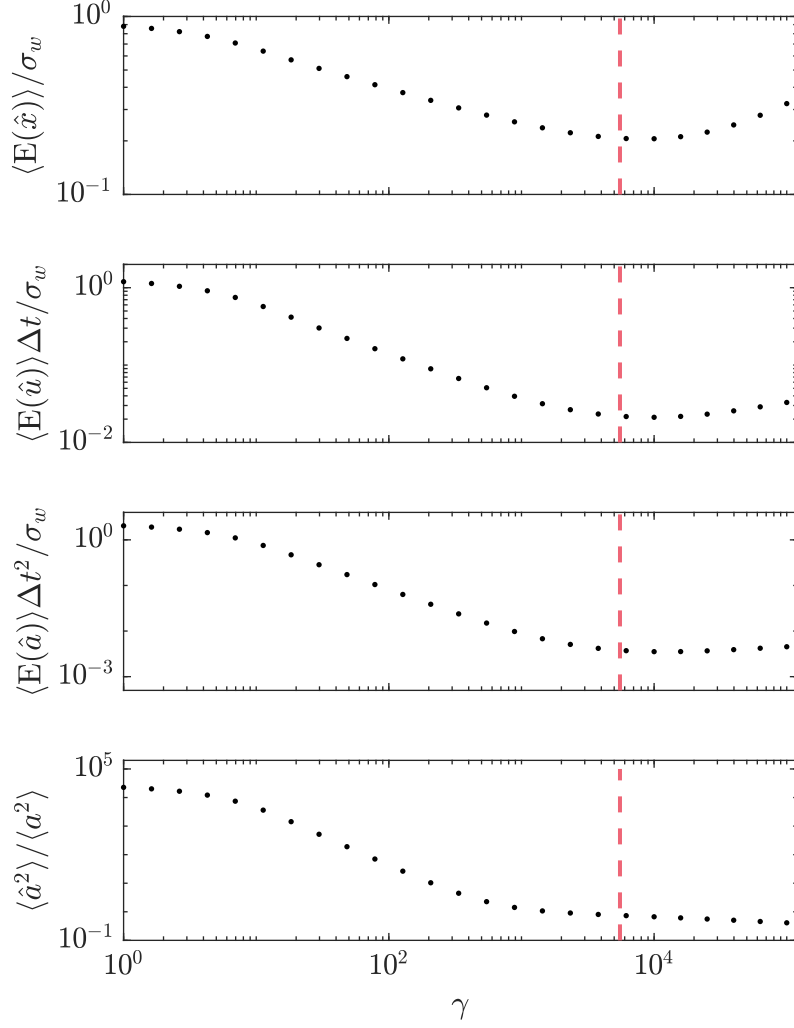


Figure 1: Normalized RMSE from IRLS-filtered trajectories as a function of sparsity penalty parameter  $\gamma$  for position (first - top), velocity (second), and acceleration (third) in comparison with reconstructed acceleration statistics as a function of  $\gamma$  (bottom). All graphs are plotted on log-log scale and the tuned  $\gamma$  value is indicated by the dash pink line. In all RMSE graphs the minima occur shortly after the exponential decay (linear in log-log scale) transition of the acceleration statistics demonstrating that tuning the IRLS filter is achievable even in the absence of ground truth data.

Guided by this sensitivity hierarchy, we adopted an iterative tuning strategy. From our grid-search, we first identified a reasonably small  $\sigma_v$ , to improve numerical stability, in which reconstruction error changed negligibly. We then varied  $\gamma$  at a higher resolution. The first three panels of Figure 1 show the resulting dependence of position, velocity, and acceleration average RMSE on  $\gamma$ . From this, we identified an appealing design point at  $\sigma_v = 2.2$  and  $\gamma = 5528.7$ , shown as the dashed pink line in Figure 1.

In practical applications, the true trajectory is not available, and therefore RMSE-based optimization is infeasible. To identify a practical tuning approach, we examined how the reconstructed acceleration standard deviation varies with  $\gamma$ . We show this trend in the final panel of Figure 1. Examination of Figure 1

(bottom) shows that the acceleration statistics decay exponentially (i.e. linear in the plotted log-space) once  $\gamma$  becomes sufficiently large. Moreover, we note that the minima in the RMSE curves all occur shortly after the transition to exponential decay. Therefore, in the absence of ground truth data, the filter could be tuned by first sweeping over  $\gamma$  to identify the region in which the acceleration statistics exhibit exponential decay. Selecting  $\gamma$  near the onset of this region yields near-optimal performance.

Finally, it is tempting to link the optimized penalty parameter back to the physical intermittency model, we solve (13) for the sparsity probability  $p_0$ . This yields the analytical mapping:

$$p_0 = \frac{e^\gamma}{e^\gamma + \sqrt{2\pi}\sigma_v} \approx 1 - \sqrt{2\pi}\sigma_v e^{-\gamma}. \quad (22)$$

Using the tuned values of  $\gamma = 5528.7$  and  $\sigma_v = 2.2$ , this relationship allows us to quantify the implied probability of jerk intermittency, providing a physical interpretation of the flow's intermittency captured by the filter. With such a large  $\gamma$ , the exponential dependency exhibited in (22) yields  $p_0$  effectively equal to 1. This result is likely non-physical with the value dominated by the relaxation of the  $\ell_0$  non-convex problem to the  $\ell_1$  convex reweighting scheme. This is noted because the derived  $\sigma_v$  and  $p_0$  can be corrupted by the nature of the convex relaxation. Relaxation from an  $\ell_0$ -norm to a reweighted  $\ell_1$ -norm materially affects the underlying model. This relaxation enables tractable solution of the optimization problem, and indeed we will show in Section 4 that the results produce a strict improvement over existing state-of-the-art methods. However, in the non-convex problem, the magnitude of non-zero components would be penalized according to a function of the form

$$\frac{\|v\|_2^2}{2\sigma_v^2} + \gamma \text{card}(v), \quad (23)$$

where the component magnitudes face relatively little penalty *after* they are determined to be non-zero. On the other hand, the relaxation penalizes components according to

$$\frac{\|v\|_2^2}{2\sigma_v^2} + \gamma \|v\|_1. \quad (24)$$

In the case of (24), the parameter  $\gamma$  imparts a heavy penalty on the absolute magnitudes of  $v$  which dwarfs the quadratic penalty and is suspected to be the root cause of the insensitivity of the performance to  $\sigma_v$  in the relaxed scheme; as  $\sigma_v$  increases the quadratic term is further reduced.

## 4.2 Trajectory Error and Reconstruction

Figure 2 illustrates a representative segment of a reconstructed particle trajectory. As shown, the underlying DNS data (solid black line) exhibits rapid, high-curvature transitions indicative of extreme acceleration events. The baseline filtering approaches tend to over-smooth these dynamic regions, failing to capture the full amplitude of the local spatial fluctuations. In contrast, the proposed IRLS filter (solid pink line) tracks the ground-truth DNS trajectory with substantially higher fidelity, particularly during sharp deviations. By relaxing the assumed Gaussian constraint on the jerk and instead penalizing via the  $\ell_1$ -norm, the IRLS approach permits the sparse, high-magnitude changes necessary to resolve these intense, intermittent events without overfitting to the high-frequency measurement noise (solid grey line).

Figure 3 shows the RMSE distributions for the proposed IRLS filter compared to discrete MLE, continuous MLE, and B-splines approaches. All filters were optimized to minimize their respective mean RMSE. Across all state variables, the IRLS method produces systematic reductions in error. Relative to all other filtering approaches, IRLS reduces RMSE by at least 9% for position, 15% for velocity, and 8% for acceleration.

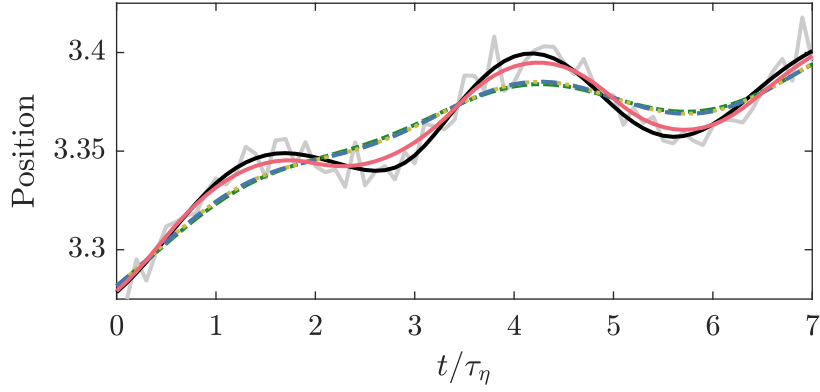


Figure 2: Example of a trajectory. Noisy position data (solid grey) is fed into the IRLS filter (solid pink), the discrete MLE filter (dashed blue), continuous MLE filter (dot-dashed green), and B-splines filter (dotted yellow). Comparing to the DNS data (solid black), the IRLS data significantly outperforms the other filters, particularly in regions of extreme accelerations.

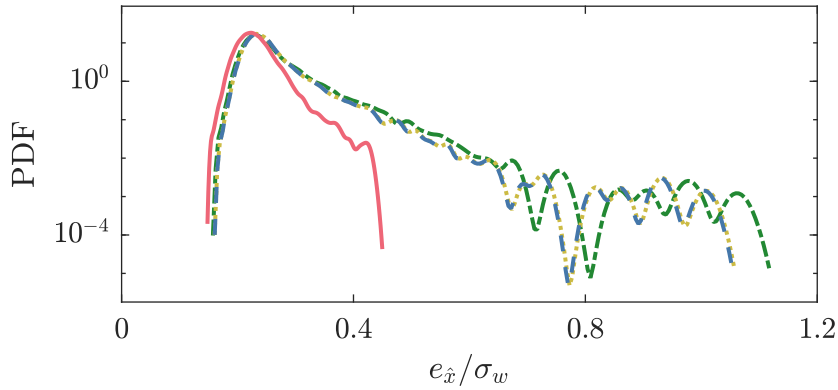


Figure 3: Error distributions for position, normalized by the standard deviation of the measurement noise  $\sigma_w$ . In all cases, the IRLS method outperforms the discrete MLE, continuous MLE, and B-splines approaches. Coloring and line styles match those used in Figure 2.

We attribute these reductions to the improved ability of the IRLS filter to capture rapid temporal fluctuations and intermittent acceleration dynamics. Figure 4 (top) shows a representative trajectory characterized by large temporal fluctuations in acceleration. Compared with the discrete MLE filter from our previous work, the IRLS reconstruction more closely follows the high-magnitude oscillations of the DNS signal, which is noticeably attenuated by the discrete MLE filter.

The distinction between the filtering methods becomes more pronounced when examining the acceleration differences, defined as  $\delta\hat{a}(\tau) = \hat{a}(t + \tau) - \hat{a}(t)$ , and shown in Figure 4 (bottom). Evaluated at the sampling interval  $\tau = \Delta t$ , these differences serve as a discrete proxy for jerk. The discrete MLE filter yields small and smoothly varying acceleration differences, indicating that rapid transitions in acceleration are strongly suppressed. In contrast, the IRLS filter produces intermittent, high-magnitude variations in  $\delta\hat{a}$ , that more closely resemble the DNS signal. Although the IRLS reconstruction exhibits amplification in the acceleration difference magnitude relative to the DNS signal, it retains the extreme, intermittent events that are largely smoothed by the discrete MLE approach.

The differences in these results can be attributed to the assumptions on the jerk distribution embedded

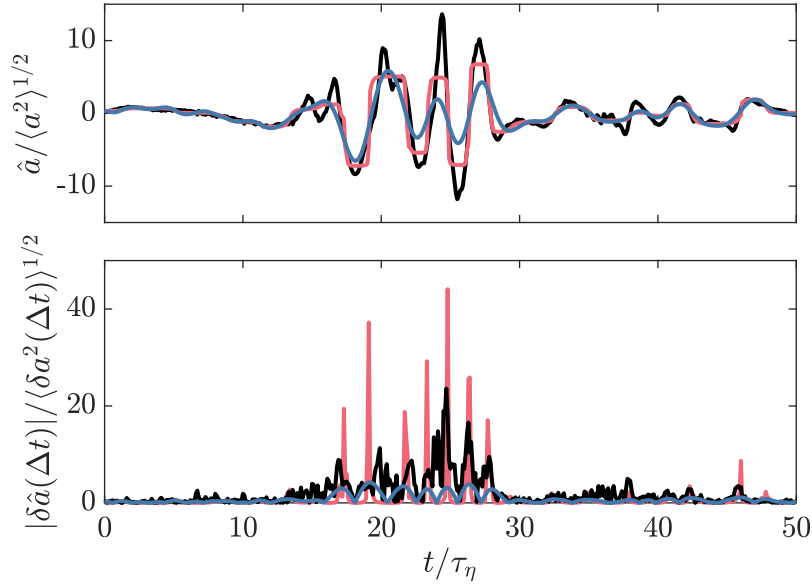


Figure 4: Acceleration time series from a representative trajectory (top) and the corresponding acceleration differences (bottom). Differences are evaluated at the sampling interval  $\Delta t$  and serve as a discrete proxy for jerk. All quantities are normalized by the standard deviation of the corresponding quantity from the DNS. Original DNS data is shown in black, the discrete MLE reconstruction in blue, and newly-developed IRLS reconstruction in pink.

in the formulation of each filter. The discrete MLE filter assumes a Gaussian jerk, and therefore penalizes large temporal variations in acceleration, leading to reduced acceleration differences. The IRLS formulation allows for sparse, high-magnitude changes in acceleration, resulting in the retention of the intermittent dynamics characteristic of turbulent flows.

### 4.3 Acceleration Statistics

Figure 5 shows the PDF of the normalized acceleration magnitude. The DNS distribution exhibits the well-known, heavy-tailed behavior, consistent with intermittent Lagrangian accelerations in turbulence. The discrete MLE, continuous MLE, and B-splines filtering approaches heavily attenuate the tails of the distribution, producing noticeably steeper decay in high volatility events. In contrast, the IRLS reconstruction closely follows the DNS distribution and substantially reduces attenuation of the tails, preserving the elevated probability of extreme events.

The distinction between filtering methods becomes most pronounced when examining the PDF of the acceleration differences evaluated at the sampling interval, shown in Figure 6. This distribution reflects rapid temporal changes in acceleration and serves as a discrete proxy for jerk. The baseline filters dramatically compress the tails of this distribution, underpredicting extreme-events by several orders of magnitude. This compression indicates that rapid transitions are over-smoothed, fundamentally altering the measured small-scale dynamics. The IRLS filter preserves a heavy-tailed distribution, recovering the probability of large acceleration increments to a far greater extent compared to the baseline filters.

Differences are observed in the core of the acceleration difference distribution, shown in the inset of Figure 6. The IRLS filter exhibits an elevated probability near zero, reflecting a tendency to produce intervals of nearly constant acceleration, punctuated by intermittent jumps. By comparison, the baseline filters slightly underpredict the probability of near-zero increments, but maintain the Gaussian-like shape of the core. The

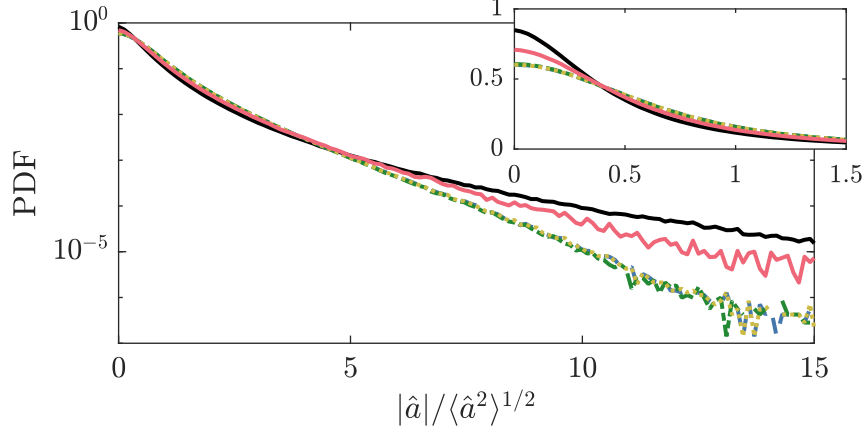


Figure 5: PDF of normalized accelerations. The DNS data exhibit the characteristic heavy-tailed structure of turbulent acceleration. The baseline MLE methods and the B-spline approach attenuate the tails of the distribution, underpredicting the probability of extreme acceleration events. In contrast, the IRLS reconstruction more closely follows the DNS distribution, demonstrating improved recovery of the heavy-tail behavior. The inset shows a zoomed view of the core of the distribution near zero acceleration, highlighting differences in the central region. Coloring and line styles match those used in Figure 2.

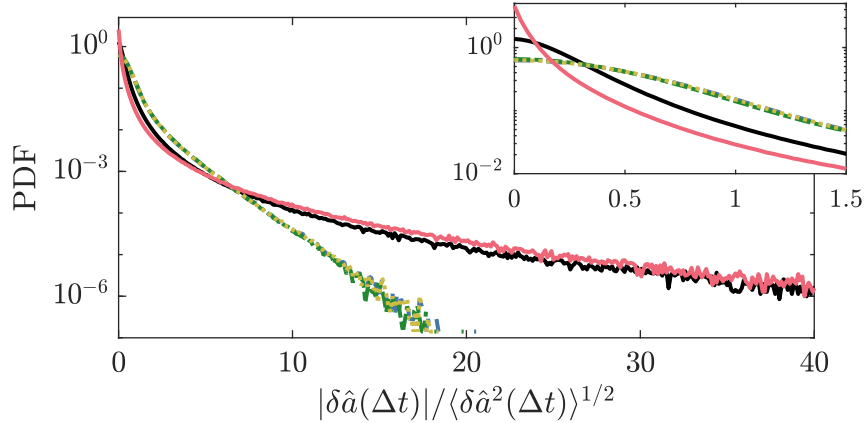


Figure 6: PDF of normalized acceleration differences evaluated at the sampling interval. The DNS distribution exhibits pronounced heavy tails. The baseline MLE and B-spline methods substantially compress the tails, underpredicting the probability of high-magnitude acceleration increments. In contrast, the IRLS reconstruction preserves a heavy-tailed structure that closely follows the DNS statistics, particularly in the extreme-event regime. The inset shows a zoomed view of the core of the distribution near zero acceleration differences. Coloring and line styles are consistent with Figure 2.

$\ell_1$  term in the IRLS objective is dominant in the small jerk regime, and it mimics a Laplace distribution as is observed in this result. This characteristic causes the IRLS PDF to deviate from the Gaussian-like shape of the truth distribution for small jerk values. The behavior highlights an inherent trade-off in trajectory reconstruction: the IRLS filter model better predicts higher volatility events and better matches the true physics of the turbulent flow, but relaxation induces distribution deviations in the near zero jerk regime. To further quantify intermittency across scales, we examine the flatness of acceleration differences as a function of separation time, shown in Figure 7. The flatness is given by  $F_{\hat{a}}(\tau) = \langle \delta \hat{a}^4(\tau) \rangle / \langle \delta \hat{a}^2(\tau) \rangle^2$ . High flatness

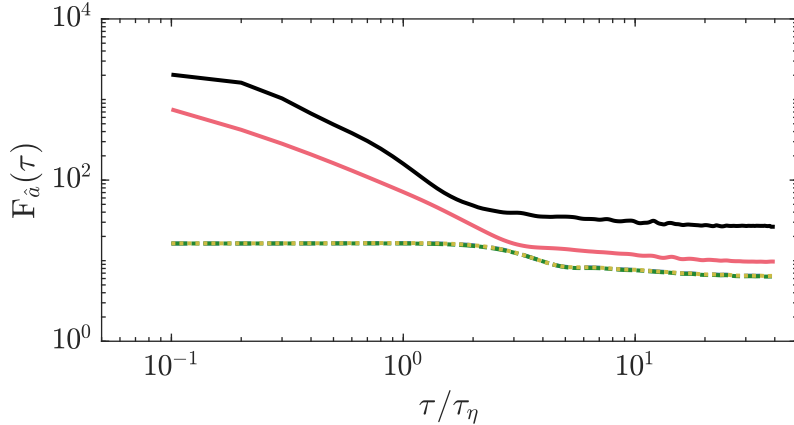


Figure 7: Flatness of normalized acceleration differences as a function of separation time. The DNS data exhibit elevated flatness values at small separations, reflecting strong intermittency and enhanced fourth-order statistics. The baseline MLE and B-spline methods substantially reduce flatness across scales, indicating suppression of high-magnitude acceleration transitions. The IRLS reconstruction maintains significantly higher flatness values that more closely follow the DNS behavior, demonstrating improved preservation of intermittent dynamics across scales. Coloring and line styles are consistent with Figure 2.

values indicate strong intermittent behavior. Across all scales, baseline filtering methods exhibit markedly reduced flatness, consistent with suppression of higher-order structure. Again, the IRLS reconstruction maintains significantly larger flatness values that more closely track the DNS behavior, demonstrating that the improved tail recovery observed in the PDF is not limited to a single scale, but persists across temporal separations.

Taken together, these results show that baseline smoothing approaches mute intermittent dynamics, whereas our newly developed IRLS filter preserves the heavy-tailed statistical structure intrinsic to turbulent flows, while maintaining low global reconstruction error.

## 5 Conclusions and Future Work

In this work, we have presented a modified MLE framework for Lagrangian particle tracking that explicitly accounts for intermittency in turbulent flows. By replacing standard Gaussian process noise assumptions with a heavy-tailed distribution modeled via a convex  $\ell_1$ -relaxation, we demonstrated a significant improvement in the recovery of flow physics. Specifically, the proposed IRLS filter successfully reconstructs the heavy tails of the acceleration PDF, which are systematically suppressed by conventional Gaussian smoothing and B-spline techniques, while maintaining position error strictly within the measurement noise floor. The results highlight improved performance in high-Reynolds-number flows when filtering strategies that are informed by richer underlying stochastic structures related to the turbulence.

Current results open several avenues for future research, particularly in establishing a rigorous link between the optimization hyperparameters and physical flow constants. While the sparsity penalty  $\gamma$  and process noise  $\sigma_v$  were tuned empirically in this study, they act as proxies for the physical intermittency and dissipation rate of the flow. Future experimental campaigns are warranted to characterize these parameters as functions of the Reynolds number ( $Re_\lambda$ ) and Stokes number ( $St$ ). We aim to develop a mapping that eliminates the need for post-hoc tuning, allowing the filter to adapt dynamically based on known flow conditions. Such a study would require an interdisciplinary approach, combining high-fidelity measurements from experimental facilities with advanced stochastic system identification.

From a theoretical perspective, the underlying dynamical model can be enriched beyond the third-order dynamics used here. As noted in the discussion, the current model assumes white process noise. However, the forces acting on a fluid particle often exhibit temporal correlations. Future iterations of this framework could incorporate colored noise models or additional physical constraints, such as damping terms or mean-field coupling, to better represent the particle’s interaction with the viscous fluid. Integrating these higher-fidelity dynamical systems into the convex optimization framework would provide a more robust connection between the mathematical solver and the Navier-Stokes physics.

Finally, this framework provides a natural foundation for real-time state estimation in autonomous systems. While the IRLS algorithm presented here is iterative and suited for post-processing, it serves as a prototype for modern “algorithm unrolling” techniques in machine learning. By unrolling the iterations of the IRLS solver into a deep neural network, it is possible to generate fixed-complexity, differentiable estimators that approximate the solution of the convex problem with millisecond latency. This translation from offline optimization to online inference has far-reaching consequences for flow control, enabling autonomous vehicles to estimate local flow structures and intermittent forcing events in real-time.

## Appendix A Error Landscapes in Filter Parameter Space

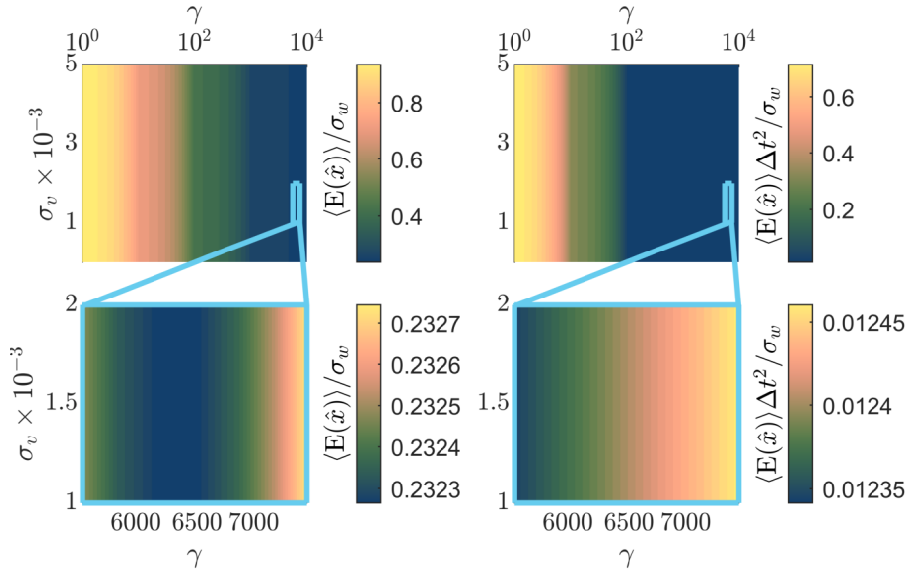


Figure 8: Hierarchical parameter tuning landscapes for position (left) and acceleration (right). The coarse parameter sweep (top) reveals that filter performance is highly sensitive to the sparsity parameter  $\gamma$  (log scale) while remaining relatively robust to changes in  $\sigma_v$  (vertical stratification). The fine-resolution search (bottom) focuses on minor variations, identifying an appealing performance configuration of  $\gamma \approx 5529$ . The persistence of the vertical banding in the fine stage confirms the filter’s robustness to process noise variance enabling a configuration with a relatively small  $\sigma_v$  values.

Figure 8 shows the RMSE landscapes in the  $(\gamma, \sigma_v)$  parameter space for both position and acceleration. The upper panels show the results of the initial coarse grid search, which reveal a distinct sensitivity hierarchy. Error gradients are primarily aligned with the  $\gamma$  axis, resulting in vertical stratification of the error surface. This indicates that reconstruction quality is predominantly driven by the sparsity enforcement ( $\gamma$ ) rather than the specific process noise width ( $\sigma_v$ ).

The lower panels in Figure 8 present the results from our fine-resolution search near the apparent

minimum. Although the optimal  $\gamma$  values differ slightly between position and acceleration, the error surface in this neighborhood is relatively flat. Across the fine-resolution sweep, the performance varies by just  $3.7 \times 10^{-7}\%$  for position and  $2.9 \times 10^{-8}\%$  for the acceleration RMSE. The persistence of vertical banding at this scale further reinforces the conclusions that the reconstruction performance is relatively insensitive to  $\sigma_v$  within the tested range.

Taken together, these results indicate that the newly proposed IRLS filter exhibits robust performance across a wide range of process noise assumptions. This hierarchical sensitivity structure simplifies practical parameter tuning in the absence of ground truth.

## References

- Toshihico Arimitsu and Naoko Arimitsu. Multifractal analysis of fluid particle accelerations in turbulence. *Physica D: Nonlinear Phenomena*, 193(1-4):218–230, 2004.
- Sathyanarayana Ayyalasomayajula, Armann Gylfason, Lance R Collins, Eberhard Bodenschatz, and Zellman Warhaft. Lagrangian measurements of inertial particle accelerations in grid generated wind tunnel turbulence. *Physical Review Letters*, 97(14):144507, 2006.
- C Beck. Lagrangian acceleration statistics in turbulent flows. *Europhysics Letters (EPL)*, 64(2):151–157, October 2003. ISSN 0295-5075, 1286-4854. doi: 10.1209/epl/i2003-00498-4.
- Christian Beck. Dynamical foundations of nonextensive statistical mechanics. *Physical Review Letters*, 87(18):180601, 2001.
- Lukas Bentkamp, Cristian C. Lalescu, and Michael Wilczek. Persistent accelerations disentangle Lagrangian turbulence. *Nature Communications*, 10(1):3550, August 2019. ISSN 2041-1723. doi: 10.1038/s41467-019-11060-9.
- Luca Biferale, Fabio Bonaccorso, Michele Buzzicotti, and Chiara Calascibetta. Turb-lagr. a database of 3d lagrangian trajectories in homogeneous and isotropic turbulence. *arXiv preprint arXiv:2303.08662*, 2024.
- Stephen Boyd, Neal Parikh, Eric Chu, Borja Peleato, and Jonathan Eckstein. Distributed optimization and statistical learning via the alternating direction method of multipliers. *Foundations and Trends® in Machine Learning*, 3(1):1–122, 2011.
- Stephen P. Boyd and Lieven Vandenbergh. *Convex Optimization*. Cambridge University Press, Cambridge, UK, 2004. ISBN 978-0521833783.
- Scott Shaobing Chen, David L Donoho, and Michael A Saunders. Atomic decomposition by basis pursuit. *SIAM review*, 40(1):33–61, 1998.
- Laurent Chevillard and Charles Meneveau. Lagrangian dynamics and statistical geometric structure of turbulence. *Physical review letters*, 97(17):174501, 2006.
- Ingrid Daubechies, Ronald DeVore, Massimo Fornasier, and C. Sinan Güntürk. Iteratively reweighted least squares minimization for sparse recovery. *Communications on Pure and Applied Mathematics*, 63(1):1–38, 2010. doi: <https://doi.org/10.1002/cpa.20303>.
- Uriel Frisch and Andreï Nikolaevich Kolmogorov. *Turbulence: the legacy of AN Kolmogorov*. Cambridge university press, 1995.

- Sebastian Gesemann. From particle tracks to velocity and acceleration fields using b-splines and penalties. *arXiv preprint*, 2015.
- Sebastian Gesemann. Trackfit: uncertainty quantification, optimal filtering and interpolation of tracks for time-resolved lagrangian particle tracking. In *14th International Symposium on Particle Image Velocimetry*, volume 1, 2021.
- Griffin M. Kearney and Makan Fardad. Optimization based data enrichment using stochastic dynamical system models. *PLOS ONE*, 19(9):1–27, 09 2024. doi: 10.1371/journal.pone.0310504. URL <https://doi.org/10.1371/journal.pone.0310504>.
- Griffin M. Kearney, Kasey M. Laurent, and Reece V. Kearney. Maximum likelihood filtering for particle tracking in turbulent flows. *Experiments in Fluids*, 65, 2024. ISSN 07234864. doi: 10.1007/s00348-024-03765-5.
- Andrey Nikolaevich Kolmogorov. The local structure of turbulence in incompressible viscous fluid for very large reynolds. *Numbers. In Dokl. Akad. Nauk SSSR*, 30:301, 1941.
- Andrey Nikolaevich Kolmogorov. A refinement of previous hypotheses concerning the local structure of turbulence in a viscous incompressible fluid at high reynolds number. *Journal of Fluid Mechanics*, 13(1): 82–85, 1962.
- Arthur La Porta, Greg A Voth, Alice M Crawford, Jim Alexander, and Eberhard Bodenschatz. Fluid particle accelerations in fully developed turbulence. *Nature*, 409(6823):1017–1019, 2001.
- AG Lamorgese, Stephen B Pope, PK Yeung, and Brian Lewis Sawford. A conditionally cubic-gaussian stochastic lagrangian model for acceleration in isotropic turbulence. *Journal of Fluid Mechanics*, 582: 423–448, 2007.
- John M. Lawson, Eberhard Bodenschatz, Cristian C. Lalescu, and Michael Wilczek. Bias in particle tracking acceleration measurement. *Exp Fluids*, 59:1–14, 2018. ISSN 07234864. doi: 10.1007/s00348-018-2622-0.
- Beat Lüthi, Arkady Tsinober, and Wolfgang Kinzelbach. Lagrangian measurement of vorticity dynamics in turbulent flow. *Journal of Fluid mechanics*, 528:87–118, 2005.
- N. Mordant, A.M. Crawford, and E. Bodenschatz. Experimental lagrangian acceleration probability density function measurement. *Physica D*, 193(1):245–251, 2004. ISSN 0167-2789. doi: <https://doi.org/10.1016/j.physd.2004.01.041>.
- Nicolas Mordant, Pascal Metz, Olivier Michel, and J-F Pinton. Measurement of lagrangian velocity in fully developed turbulence. *Phys Rev Lett*, 87(21):214501, 2001. doi: 10.1103/PhysRevLett.87.214501.
- AM Reynolds. Superstatistical mechanics of tracer-particle motions in turbulence. *Physical review letters*, 91(8):084503, 2003.
- B. L. Sawford, P. K. Yeung, M. S. Borgas, P. Vedula, A. La Porta, A. M. Crawford, and E. Bodenschatz. Conditional and unconditional acceleration statistics in turbulence. *Phys Fluids*, 15(11):3478–3489, 2003. ISSN 1070-6631. doi: 10.1063/1.1613647.
- BL Sawford. Reynolds number effects in lagrangian stochastic models of turbulent dispersion. *Physics of Fluids A: Fluid Dynamics*, 3(6):1577–1586, 1991.

Robert Tibshirani. Regression shrinkage and selection via the lasso. *Journal of the Royal Statistical Society: Series B (Methodological)*, 58(1):267–288, 1996.

Greg A. Voth, A. La Porta, Alice M. Crawford, Jim Alexander, and Eberhard Bodenschatz. Measurement of particle accelerations in fully developed turbulence. *J Fluid Mech*, 469:121–160, 2002. doi: 10.1017/S0022112002001842.